

THERMAL BEHAVIOR OF ANTIMONY NANOWIRE ARRAYS EMBEDDED IN ANODIC ALUMINUM OXIDE TEMPLATE

X. Zhang¹, Y. Ding², Y. Zhang¹, Y. Hao¹, G. Meng^{1*} and L. Zhang¹

¹Key Laboratory of Materials Physics, and Anhui Key Laboratory of Nanomaterials and Nanostructures, Institute of Solid State Physics, Chinese Academy of Sciences, Hefei 230031 P. R. China

²Hefei National Laboratory for Physical Science at Microscale, Structure Research Laboratory, University of Science and Technology of China, Hefei 230026 P. R. China

Highly oriented single crystal antimony nanowire arrays have been synthesized within anodic aluminum oxide (AAO) template by pulsed electrodeposition. Thermal behavior and oxidation analysis of the antimony nanowires have been investigated by means of thermogravimetry and differential scanning calorimetry in Ar and air atmosphere, respectively. Compared to bulk antimony, the antimony nanowires exhibit a lower sublimation temperature at 496.4°C. Evident oxidation of the Sb nanowires occurs at 429.8°C in air atmosphere and α -Sb₂O₄ nanowires have been obtained as the oxidation product. The results indicate that the sublimation and the oxidation of the antimony nanowires in the AAO template is a slow multi-step process. The present results are of relevance when processing antimony nanowires for thermoelectric applications at high temperatures.

Keywords: antimony nanowires, TEM, thermal analysis, thermoelectric material

Introduction

Thermoelectric materials, which convert energy between heat and electricity directly, have been always fascinating because their great potential for refrigeration and power generation applications. Figure-of-merit (ZT), given by $ZT=S^2\sigma T/\kappa$, represents the relative magnitudes of thermal and electrical cross-effect transport in materials: larger ZT signifies efficient conversion of thermal to electric power. Where the factors are, the Seebeck coefficient (S), the electrical conductivity (σ) and thermal conductivity (κ), respectively [1]. Low dimensional nanostructures give rise to new opportunities for developing large ZT thermoelectric materials owing to decreased lattice thermal conductivity, improved carrier mobility, and/or a high density of state just above Fermi level [2].

Antimony (Sb) is a semimetal with a narrow energy overlap of 180 meV between the L-point of conduction band and T-point of valence band at 4.2 K, long mean free path of a few micrometers, larger de Broglie wavelength of 40 nm [3]. If Sb can be synthesized as nanowires, enhanced density of states due to quantum confinement effects will elevate S without decreasing σ , strong ballistic effects may be observed due to long electron mean free path, boundary scattering on the nanowire wall will reduce the value of κ more than that of σ . Therefore, Sb nanowires are expected to play an important role for high efficiency thermoelectric applications. In addition, many antimonides are also widely used as thermoelectric

materials, such as Bi_{1-x}Sb_x [1, 4], CoSb₃ [5], β -Zn₄Sb₃ [6–8], and Sb₂Te₃ [9]. Although the electronic properties of one-dimensional nanostructured materials have been intensively studied, there are very few reports about thermal properties of these materials, which are important for both basic research and possible applications [10–13].

In this paper, we have synthesized highly oriented single crystalline Sb nanowire arrays within the nanochannels of anodic aluminum oxide (AAO) template using pulsed electrodeposition, and investigated their thermal properties including sublimation, oxidation, and enthalpy change of the Sb nanowire arrays. Microstructures of the Sb nanowires and their oxidation product have been investigated by X-ray diffraction (XRD) and transmission electron microscopy (TEM) analysis. The present work has evaluated the thermal stability of the Sb nanowire arrays embedded in the AAO template and may provide some interesting data for exploring potential applications of the Sb nanowires on high temperature thermoelectric nanodevices.

Experimental

Synthesis of Sb nanowires embedded in the nanochannels of AAO template

AAO templates were prepared by using a two-step anodization process as described previously [14]. After the

* Author for correspondence: gwmeng@issp.ac.cn

second anodization, the aluminum substrate at the bottom was removed in a saturated SnCl_4 solution. Then the alumina barrier layer was dissolved in 6 mass% phosphoric acid solution at 30°C for 1.5 h to get the through-pore AAO template with the pore diameter of about 50 nm. A layer of Au with about 200 nm in thickness was sputtered onto the bottom side of the AAO template to serve as working electrode. The Sb plating solution consists of 0.02 M SbCl_3 , 0.1 M $\text{C}_6\text{H}_8\text{O}_7\text{-H}_2\text{O}$ and 0.05 M $\text{K}_3\text{C}_6\text{H}_5\text{O}_7\text{-H}_2\text{O}$. The initial pH was adjusted to 2.0 by adding appropriate amount of 5 M H_2SO_4 solution. The pulsed electrodeposition was performed at 12°C, to get single crystal Sb nanowire arrays [15].

Thermal analysis

Thermogravimetry (TG) and differential scanning calorimetry (DSC) analyses of the samples were carried out on a Shimadzu TGA-50H thermogravimetry and a DSC-50 Shimadzu differential scanning calorimetry. For TG analysis, records were obtained with a heating rate of $10^\circ\text{C min}^{-1}$ under dynamic air and Ar from 100 to 1000°C in an open alumina crucible, respectively. The sample mass was about 5 mg. Meanwhile AAO template sputtered with Au film of 3.587 mg was analyzed in Ar atmosphere in the same temperature range as reference. For DSC analysis, samples about 1.5 mg were weighed onto an open platinum crucible. Samples were also analyzed in Ar and air atmosphere respectively, with a heating rate of $10^\circ\text{C min}^{-1}$ from 100 to 650°C .

Structural characterization

The as-electrodeposited products and the residue of DSC analysis in air atmosphere were characterized by a rotating anode X-ray powder diffraction (XRD, D/MAX-Ra) with CuK_α radiation ($\lambda=1.5418 \text{ \AA}$). Microstructures of these nanowires were characterized using transmission electron microscopy (TEM, JEM 200CX) and high-resolution TEM (HRTEM, JEOL 2010). For TEM analysis, the specimens were prepared by dissolving the AAO template with a 5 mass% NaOH solution, dispersing the nanowires in ethanol by ultrasonic cleaning. Then drops of the solution were dripped onto copper grids coated with holey carbon film.

Results and discussion

The characterization of the as-electrodeposited nanowire arrays

An X-ray diffraction pattern of the Sb nanowire arrays embedded in the nanochannels of AAO template

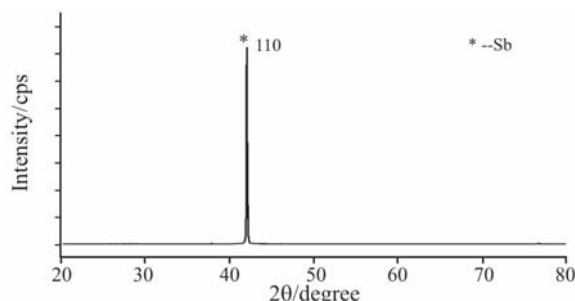


Fig. 1 XRD pattern of the synthesized nanowire arrays

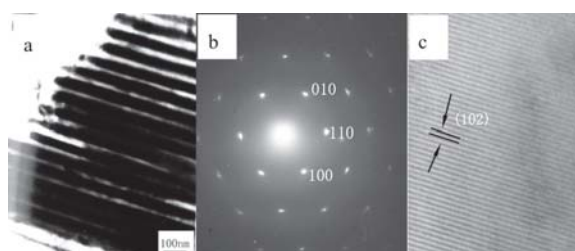


Fig. 2 a – a typical TEM image of Sb nanowires, b – SAED pattern from one of the nanowires in (a), c – high resolution TEM image of the nanowire

is shown in Fig. 1. It can be seen that there is a very sharp diffraction peak at $2\theta=41.98^\circ$ corresponding to (110) crystal plane of Sb, and the other diffraction peaks are very weak, indicating that the Sb nanowires deposited in the template grow perpendicularly to (110) plane.

Typical TEM image the nanowires (Fig. 2a) indicates that the diameter of synthesized nanowires is about 50 nm. Figure 2b shows the selected area electron diffraction (SAED) pattern of a single Sb nanowire, the diffraction spots of (100), (110) and (010) correspond to single crystal hexagonal packed structure of antimony. As shown in Fig. 2c, lattice-resolved HRTEM image of Sb (102) plane reveals high crystalline quality of the Sb nanowires.

Thermal analysis

Figure 3 shows the TG curve of the gold sputtered AAO template. The curve was obtained in Ar atmosphere, showing three obvious mass loss steps in the curve. Because there is no apparent mass loss for the AAO template in this temperature range, this mass loss can be assigned to the release of the thin gold film. The melting point of the gold film shifts to a lower temperature at about 844.2°C in comparison with that of bulk gold [16]. The main mass loss in the temperature range 844.2 and 909.1°C caused by the evaporation of the molten gold is about 3.5%. And the melting rate of the gold particles increases with further elevating temperature.

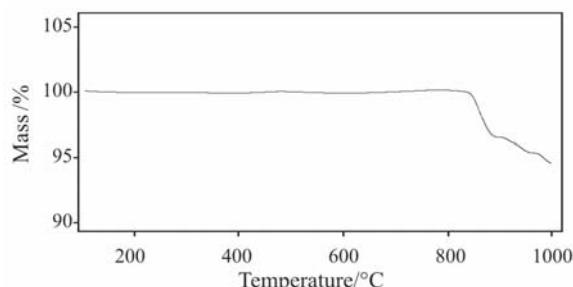


Fig. 3 TG curve for the AAO template sputtered with a golden film

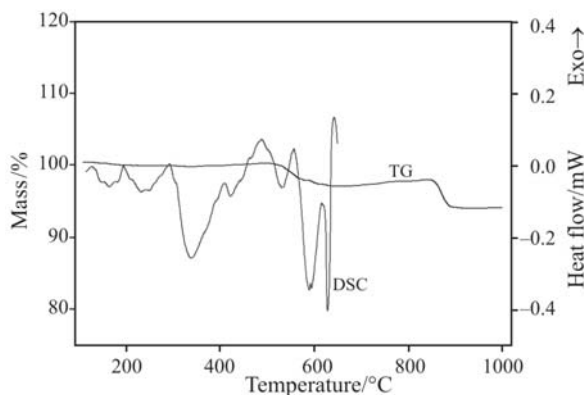


Fig. 4 TG and DSC curves of the Sb nanowire arrays in Ar atmosphere

Figure 4 exhibits the TG curve of the Sb nanowire arrays embedded in the AAO template in Ar atmosphere, two obvious mass loss steps can be observed here. The first mass loss is 3.2% located in between 528.5 and 642.6°C, which is associated with the sublimation of Sb [17]. The second mass loss is 3.8% located in the temperature range from 861.0 to 914.4°C, which may be due to the evaporation of the molten gold film used as electrode during electro-deposition of the nanowires. This result is in consistency with TG result of the template sputtered with gold layer but without Sb nanowires.

DSC curve (Fig. 4) of the same sample displays multiple weak endothermic peaks. The endothermic peaks from 194.4 to 408.0°C are caused by the release of water, coming from the hydroxyl group that is originated from anodization process [18]. The onset sublimation temperature of the Sb nanowires embedded in AAO template is about 496.4°C, indicating that the sublimation temperature of the Sb nanowires is shifted to a lower temperature compared with that of bulk Sb [17]. The broad endothermic peak from 496.4 to 644.2°C, which are split into three peaks, can be assigned to the sublimation of antimony in three stages. The first stage of lower temperature is related to the sublimation of Sb at the grain boundaries of the Sb nanowires [19]. Following this, more and more Sb

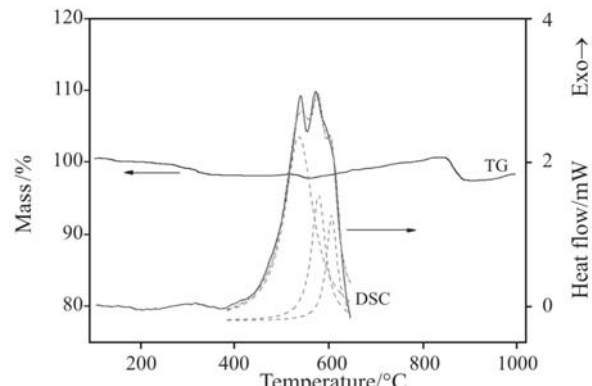


Fig. 5 TG and DSC curves of the Sb nanowire arrays in air atmosphere

sublimes. Finally, the sublimation of the middle Sb nanowires occurs. The enthalpy changes of three stages are about 3.61, 11.12 and 3.38 J g⁻¹, respectively. Due to the restriction of the instrument measurement range, the whole enthalpy change in the sublimation reaction cannot be obtained.

As shown in Fig. 5, the TG curve of the Sb nanowires obtained in air environment shows multiple stages. The first stage is a 1.9% mass loss between 156.9 and 465.5°C, which may be due to the release of water, in consistent with the analysis in Ar condition. Different from the curve in Ar atmosphere, there are two stages in the temperature range from 465.5 to 592.1°C for the curve obtained in air atmosphere. This phenomenon can be explained as follows. Firstly, the oxidization of surface antimony leads to mass gain, whereas the sublimation of Sb nanowires causes the mass loss, the net effect of the above two processes produces these two stages. Subsequently, there is an obvious mass gain about 2.9% from 592.1 to 858.1°C, which is mainly due to the oxidation of Sb in the AAO template. The broad mass gain temperature range may mean that the oxidation of the Sb nanowires is a slow process. Similar to the curve in Ar atmosphere, there also exists a mass loss stage of the gold film for the curve in air atmosphere. Following this, there is an obvious mass gain till 957.8°C. The percentage of the mass loss of Au in air is smaller than that in Ar, which may be due to the partial oxidation of gold in air.

As shown in Fig. 5, there is an obvious exothermic peak in the DSC curve for the Sb nanowire arrays in air atmosphere. The onset oxidation temperature of the Sb nanowire arrays embedded in the AAO template is about 429.8°C. The broad strong exothermic peak means that there is a slow oxidation process for the Sb nanowire arrays in air atmosphere. Similar to the sublimation of the Sb nanowires in Ar atmosphere, the oxidation of the Sb nanowires can be fitted into three stages. The lower temperature step is re-

lated to the oxidation of Sb at the grain boundaries of the Sb nanowire arrays. Secondly, more and more Sb is oxidized with increasing temperature. Finally, the oxidation of Sb in the middle of nanowires occurs at higher temperature [19]. The enthalpy change of each stage is about 299.25, 97.58 and 61.94 J g⁻¹, respectively. This confirms that the main chemical reaction of the Sb nanowire arrays in air atmosphere is an oxidation process, while the sublimation of the Sb nanowire arrays is very weak. Unfortunately, the whole enthalpy change in the oxidation reaction cannot be obtained because of the restriction of the instrument measurement range.

Structural characterization of the residue after DSC analysis in air atmosphere

XRD pattern of the residue after DSC analysis in air atmosphere reveals that the residue is dehydrated orthorhombic α -Sb₂O₄ (Fig. 6). The structure is in $C_{2v}^0/P\text{na}2_1$ space group, and the parameters of the unit cell are $a=4.804\text{ \AA}$, $b=5.424\text{ \AA}$ and $c=11.76\text{ \AA}$, respectively [20].

Typical bright field TEM image of and high-resolution TEM image of the nanowires with diffraction pattern are shown in Fig. 7. Intense diffraction spots

of (002), (200) and (202) lattice planes are characteristics of the orthorhombic structure of α -Sb₂O₄. It should be noted that some inhibited diffraction spots appear here, i.e. (001) lattice plane. From the HRTEM image of the same nanowire, the (001) lattice fringe with lattice spacing around 1.2 nm can be clearly observed, being in consistence with the diffraction pattern.

Conclusions

Systemic thermal analysis of Sb nanowires embedded in the AAO template has been investigated in Ar and air atmosphere, respectively. The results indicate that single crystalline Sb nanowires embedded in the AAO template possess excellent thermal stability below 400°C. DSC and TG analyses show that obvious sublimation of the Sb nanowires occurs up to 496.4°C in Ar atmosphere, while oxidation process dominates from 429.8°C in air ambience, accompanied with minute sublimation. After analysis in air atmosphere, the Sb nanowires with hexagonal structure were oxidized into α -Sb₂O₄ nanowires with orthorhombic structure. The results are in good agreement with that of the thermal analysis. This research will outline the optimal operation temperature range of the Sb nanowire arrays in thermoelectric device.

Acknowledgements

This work was financially supported by the National Science Fund for Distinguished Young Scholars (Grant No. 50525207), the Natural Science Foundation of China (Grant No. 10374092), and the National Major Project of Fundamental Research: Nanomaterials and Nanostructures (Grant No. 2005CB623603).

References

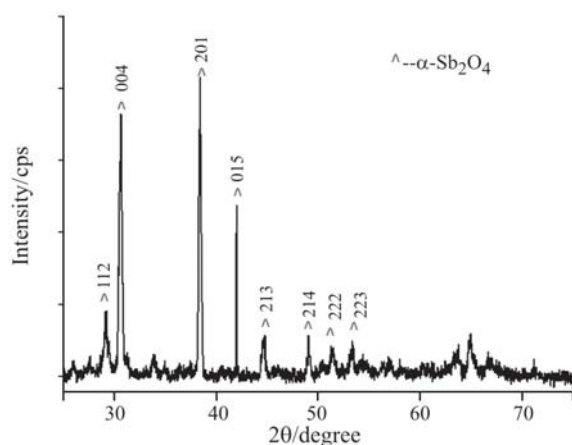


Fig. 6 XRD pattern of the residue after measurement in air atmosphere

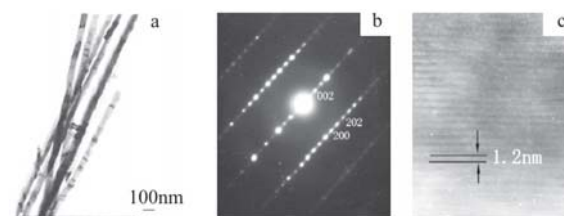


Fig. 7 a – TEM image of the α -Sb₂O₄ nanowires obtained after analysis in air atmosphere, b – SAED pattern taken from the nanowire shown in (a), c – high resolution TEM image of a single α -Sb₂O₄ nanowire

- 1 Y. M. Lin, O. Rabin, S. B. Cronin, J. Y. Ying and M. S. Dresselhaus, *Appl. Phys. Lett.*, 81 (2002) 2403.
- 2 L. D. Hicks, T. C. Harman and M. S. Dresselhaus, *Appl. Phys. Lett.*, 63 (1993) 3230.
- 3 L. R. Windmiller, *Phys. Rev.*, 149 (1966) 472.
- 4 T. Kyratsi, D. Y. Chung and M. G. Kanatzidis, *J. Alloys Compd.*, 338 (2002) 36.
- 5 T. Shimozaki, K. Kim, T. Iwata, T. Okino and C.G. Lee, *Mater. Trans.*, 43 (2002) 2609.
- 6 J. Nylen, M. Andersson, S. Lidin and U. Haussmann, *J. Am. Chem. Soc.*, 126 (2004) 16306.
- 7 Y. Mozharivskyj, A. O. Pecharsky, S. Bud'ko and G. J. Miller, *Chem. Mater.*, 16 (2004) 1580.
- 8 L. T. Zhang, M. Tsutsui, K. Ito and M. Yamaguchi, *Thin Solid Film*, 443 (2003) 84.

- 9 C. G. Jin, G. Q. Zhang, T. Qian, X. G. Li and Z. Yao, *J. Phys. Chem. B*, 109 (2005) 1430.
- 10 J. Heremans, C. M. Thrush, Y. M. Lin, S. B. Cronin and M. S. Dresselhaus, *Phys. Rev. B*, 63 (2001) 085406.
- 11 L. D. Hicks and M. S. Dresselhaus, *Phys. Rev. B*, 47 (1993) 16631.
- 12 D. Y. Li, Y. Y. Wu, P. Kim, L. Shi, P. D. Yang and A. Majumdar, *Appl. Phys. Lett.*, 83 (2003) 2934.
- 13 H. Matsushita, E. Hagiwara and A. Katsui, *J. Mater. Sci.*, 39 (2004) 6299.
- 14 H. Masuda and K. Fukuda, *Science*, 268 (1995) 1466.
- 15 Y. Zhang, G. H. Li, Y. C. Wu, B. Zhang, W. H. Song and L. D. Zhang, *Adv. Mater.*, 14 (2002) 1227.
- 16 P. Buffat and J-P. Borel, *Phys. Rev. A*, 13 (1976) 2287.
- 17 B. V. L'vov and A. V. Novichikhin, *Thermochim. Acta*, 290 (1997) 239.
- 18 O. Jessensky, F. Muller and U. Gosele, *Appl. Phys. Lett.*, 72 (1998) 1173.
- 19 A. Kolmakov, Y. X. Zhang and M. Moskovits, *Nano Lett.*, 3 (2003) 1125.
- 20 Z. L. Zhang, *J. Mater. Res.*, 17 (2002) 1698.

Received: March 25, 2005

Accepted: December 20, 2006

OnlineFirst: April 29, 2007

DOI: 10.1007/s10973-005-7017-9